İstatistikçiler Dergisi: İstatistik & Aktüerya

Journal of Statisticians: Statistics and Actuarial Sciences

IDIA 19, 2026, 71–92

Geliş/Received: 12.07.2026, **Kabul**/Accepted: 09.08.2026

Araştırma Makalesi / Research Article

An attribute control chart for compound Weibull distribution based on median

Canan Hamurkaroğlu

Karabük University,
Department of Actuerial Science
Karabük, Türkiye
cananhamurkaroglu@karabuk.edu.tr
0000-0002-8537-513X

Nazan Danacıoğlu

Sinop University
Department of Data Science and Analytics
Sinop, Türkiye
nazand@sinop.edu.tr
0000-0001-8014-6920

Abstract

This study proposes an attribute control chart for the compound Weibull distribution based on a single sampling plan under a time-truncated life test to monitor failure rates. To provide a more reliable representation of process deterioration in right-skewed lifetime distributions, process shifts are defined in terms of the median lifetime. The performance of the proposed attribute control chart is evaluated under different in-control average run length values, process shift magnitudes, and sample sizes. In addition, the performance of the chart is assessed by calculating the expected average run length and expected quadratic loss values. Design tables are constructed and interpreted by considering different combinations of the compound Weibull distribution shape parameters, sample sizes, average run length values, and process shift magnitudes. Finally, data generated from the compound Weibull distribution are used to demonstrate the effectiveness of the proposed np attribute control chart in detecting changes in the median lifetime and monitoring product quality under a time-truncated life test, and the proposed approach is illustrated through representative example scenarios. Overall, the results demonstrate that the proposed attribute control chart is applicable to processes in which product lifetimes follow the Compound Weibull distribution and provides an effective tool for monitoring process shifts.

Keywords: Average run length, Compound Weibull distribution, expected average run length, expected quadratic loss, Monte Carlo simulation, standard deviation of the run length, time-truncated life test.

Öz

Bileşik Weibull dağılımı için medyan yaşam süresine dayalı niteliksel kontrol kartı

Bu çalışmada, tek örnekleme planına dayalı ve zaman kısıtlı yaşam testi altında arıza oranlarını izlemek amacıyla bileşik Weibull dağılımı için nitelik kontrol kartı ele alınmıştır. Süreç kaymaları, *sağa çarpık yaşam süresi dağılımlarında süreç bozulmasını daha güvenilir biçimde yansıtabilmek amacıyla, medyan yaşam süresi üzerinden tanımlanmıştır. Önerilen nitelik kontrol kartının performansı, farklı kontol içi ortalama işletim uzunluğu değerleri, kayma parametreleri ve örneklem büyüklükleri altında incelenmiştir. Ayrıca, beklenen ortalama işletim uzunluğu, karesel kayıp fonksiyonu değerleri de hesaplanarak kartın performansı değerlendirilmiştir. Bileşik Weibull dağılımı şekil parametreleri, örneklem büyüklükleri, ortalama işletim uzunluğu ve süreç kayma büyüklüklerine ilişkin farklı kombiansyonlar ele alınarak tasarım tabloları hazırlanmış ve yorumlanmıştır. Niteliksel np kontrol kartının medyan yaşam süresindeki değişimleri belirlemede ve zaman kısıtlı yaşam testi altında ürün kalitesini izlemede etkili olduğunu göstermek için bileşik Weibull verisi türetilmiş, örnek senaryolar verilerek açıklanmıştır. Genel olarak, elde edilen bulgular önerilen nitelik kontrol kartının yaşam sürelerinin bileşik Weibull dağılımını izlediği süreçlerde uygulanabilir olduğunu ortaya koymakta ve süreç kaymalarının izlenmesinde etkili bir araç sunduğunu göstermektedir.*

Anahtar Kelimeler: *Ortalama işletim uzunluğu,bileşik Weibull dağılımı, beklenen ortalama işletim uzunluğu, beklenen karesel kayıp, Monte Carlo simülasyonu, işletim uzunluğunun standart sapması, zaman kısıtlı yaşam testi.*

1. Introduction

Statistical process control (SPC) employs control charts as one of the most effective tools for monitoring process stability and ensuring consistent product quality. These charts distinguish between common-cause variation, which is inherent in a stable process, and special-cause variation, which indicates process deterioration and requires corrective action. Depending on the type of quality characteristic under investigation, control charts are generally classified into variable charts for continuous measurements and attribute charts for discrete quality characteristics. In reliability-related applications, product lifetime is the primary quality characteristic, and the underlying lifetime distributions are typically positively skewed with long right tails [1]. Moreover, lifetime experiments are frequently conducted under time and cost constraints, making it impractical to observe the exact failure times of all test units. As a result, considerable research has focused on developing attribute control charts based on time-truncated life tests under a wide range of lifetime distributions and sampling schemes, including single, double, repetitive, multiple dependent state, sequential, Type I, Type II, and hybrid sampling plans.

The theoretical foundation of control charts is rooted in statistical hypothesis testing. Within this framework, a Type I error occurs when an in-control process is incorrectly identified as out of control, whereas a Type II error arises when a genuine process shift remains undetected. The effectiveness of a control chart is therefore commonly assessed through the Average Run Length (ARL), which reflects the expected number of samples collected before an out-of-control signal is issued and is directly determined by the probabilities of Type I and Type II errors. Although ARL is the most widely used performance criterion, it does not fully characterize the performance of a control chart under parameter uncertainty or varying process conditions. For this reason, complementary measures such as the Expected Average Run Length (EARL), Expected Quadratic Loss (EQL), and Standard Deviation of the Run Length (SDRL) are frequently considered to provide a more comprehensive evaluation of the overall performance and robustness of attribute control charts.

Many studies have been conducted on attribute control charts under truncated life testing in recent years. The existing literature includes numerous control chart designs developed for different lifetime distributions and censoring schemes. Although a variety of lifetime distributions have been investigated, studies considering the Compound Weibull (CW) distribution with process shifts defined in terms of the median lifetime are still limited. On the other hand, comprehensive evaluations of attribute control chart performance using multiple performance measures, rather than relying solely on ARL, remain limited.

Numerous attribute control charts have been developed for truncated life tests by considering different lifetime distributions, censoring schemes, and sampling strategies. Shafqat et al. [2] proposed a Shewhart-type attribute control chart based on a single sampling plan for Burr X, Burr XII, inverse Gaussian, and exponential lifetime distributions. Adeoti et al. [3] developed an attribute control chart using repetitive sampling to monitor the mean lifetime of products following the Rayleigh distribution under truncated life tests. Kavitha and Gunasekaran [4] introduced an attribute control chart for monitoring the median lifetime of products following the Exponentiated–Rayleigh distribution under hybrid censoring. Similarly, Kolli et al. [5] designed an attribute control chart for the new Lomax–Rayleigh distribution under time-truncated life tests, while Nanthakumar and Kavitha [6] and Saha et al. [7] proposed attribute control charts for the inverse Rayleigh, generalized Rayleigh, and Rayleigh distributions under different censoring frameworks.

Weibull-based lifetime models have also attracted considerable attention in the literature. Abd Elrazik EM [8] proposed an attribute control chart for the Weibull–Pareto distribution under truncated life testing. AL-Marshadi et al. [9] developed a time-truncated attribute control chart for the neutrosophic Weibull distribution within the framework of neutrosophic statistics. Aslam et al. [10] constructed an attribute control chart for the Weibull distribution under hybrid censoring, whereas Aslam and Jun [11] extended the application of truncated life test-based attribute control charts to non-normal lifetime distributions, including the Weibull distribution. Baklizi et al. [12] proposed an attribute control chart for the inverse Weibull distribution, while Khan et al. [13] and Khan et al. [14] developed variable and mixed control charts, respectively, for monitoring processes under time-truncated life testing based on the Weibull distribution.

Sampling strategies have likewise received significant attention as a means of improving monitoring efficiency. Aldosari et al. [15] incorporated multiple dependent state repetitive sampling into an attribute control chart, whereas Aslam et al. [16] developed a repetitive sampling-based attribute control chart for the Birnbaum–Saunders distribution.

A wide range of additional lifetime distributions has also been considered in the development of attribute control charts. Balamurali and Jeyadurga [17] proposed an attribute np control chart based on multiple deferred state sampling for monitoring the mean lifetime of products under truncated life tests and also extended this approach to the second-kind Pareto distribution. Gokila and Sheik Abdullah [18] introduced a time-efficient attribute control chart for the Exponential–Poisson distribution and subsequently extended it to the exponentiated Exponential–Poisson distribution under hybrid censoring [19]. Gunasekaran [20] proposed an attribute control chart for the exponentiated exponential distribution under hybrid censoring. Rao et al. [21] introduced an attribute control chart for the exponential inverse Kumaraswamy distribution under time-truncated life testing, while Kavitha et al. [22] designed a survival test-based attribute control chart for the exponential distribution under Type-I censoring. Additional contributions include attribute control charts for the inverse Kumaraswamy [23], exponentiated half-logistic [24], exponential Fréchet [25], Type-II generalized log-logistic [26], log-logistic [27], Dagum [28], generalized half-normal [29], and second-kind Pareto distributions [30]. In addition, Hag et al. [31] compared the ARL performance of one-sided and two-sided Shewhart control charts based on the conditional expected value with that of the corresponding attribute control charts.

In this study, the CW distribution is adopted as the product lifetime model, and an attribute np control chart for monitoring the median lifetime is developed under a time-truncated life test using a single sampling plan. The control limits and control chart constants are determined to achieve a specified in-control Average Run Length (ARL_0). The out-of-control performance of the proposed chart is evaluated by calculating the corresponding ARL_1 values for different median shift magnitudes. In addition, the performance of the proposed chart is comprehensively assessed using the ARL, EARL, EQL, and SDRL under various combinations of shape parameters and sample sizes. The proposed framework provides a practical and distribution-specific approach for designing and evaluating attribute control charts for lifetime data following the CW distribution under time-truncated life testing.

2. Compound Weibull distribution

When the quality characteristic of a product is its lifetime, it is reasonable to model the failure time using skewed distributions. For this purpose, a variety of lifetime distributions have been proposed in the literature. CW distribution is one of the distributions commonly used for modeling lifetime data.

Let T be a random variable representing the failure time of a product. If $T \sim \mathrm{CW}(\alpha, \gamma, \delta)$, the probability density function, the cumulative distribution function, mean and median are given, respectively, by [32], as follows:

Let $T \sim CW(\alpha, \gamma, \delta)$

$$f(t; \alpha, \gamma, \delta) = \frac{\alpha\gamma\delta^{\gamma} t^{\alpha-1}}{(t^{\alpha}+\delta)^{\gamma+1}} \qquad t > 0, \quad \alpha, \gamma, and\ \delta > 0 \tag{1}$$

In Equation (1), α and γ are the shape parameter and δ is the scale parameter.

$$F_T(t) = 1 - \frac{\delta^{\gamma}}{(t^{\alpha}+\delta)^{\gamma}}; \qquad t > 0, \ \alpha, \gamma, and\ \delta > 0 \tag{2}$$

The first moment of the origin is given by,

$$\mu = \frac{\delta^{\frac{1}{\alpha}}\Gamma\left(\gamma-\frac{1}{\alpha}\right)\Gamma\left(\frac{1}{\alpha}+1\right)}{\Gamma(\gamma)} \tag{3}$$

and median is given by,

$$m = \sqrt[\alpha]{\frac{\sqrt[\gamma]{2}-1}{\delta^{-1}}} = \left[\delta(2^{\frac{1}{\gamma}} - 1)\right]^{\frac{1}{\alpha}} \tag{4}$$

Reliability function $R(t)$ and hazard rate function $h(t)$ are given by, respectively,

$$R(t) = \frac{\delta^{\gamma}}{(\delta+t^{\alpha})^{\gamma}}, \qquad h(t) = \frac{\alpha\gamma t^{\alpha-1}}{\delta+t^{\alpha}}. \tag{5}$$

Figure 1 shows the hazard function, $h(t)$ and;

(1) $h(t)$ is a decreasing function of at $\alpha < 1$.

(2) $h(t)$ is approximately constant function of at $\alpha = 1$.

(3) $h(t)$ is a unimodal shaped when $\alpha > 1$.

Figure 1 illustrates that, for the fixed parameter values of δ = 1 and γ = 1, different values of the shape parameter α produce different hazard rate patterns, including decreasing, approximately constant, and unimodal shapes. This example demonstrates the flexibility of the hazard function with respect to α.

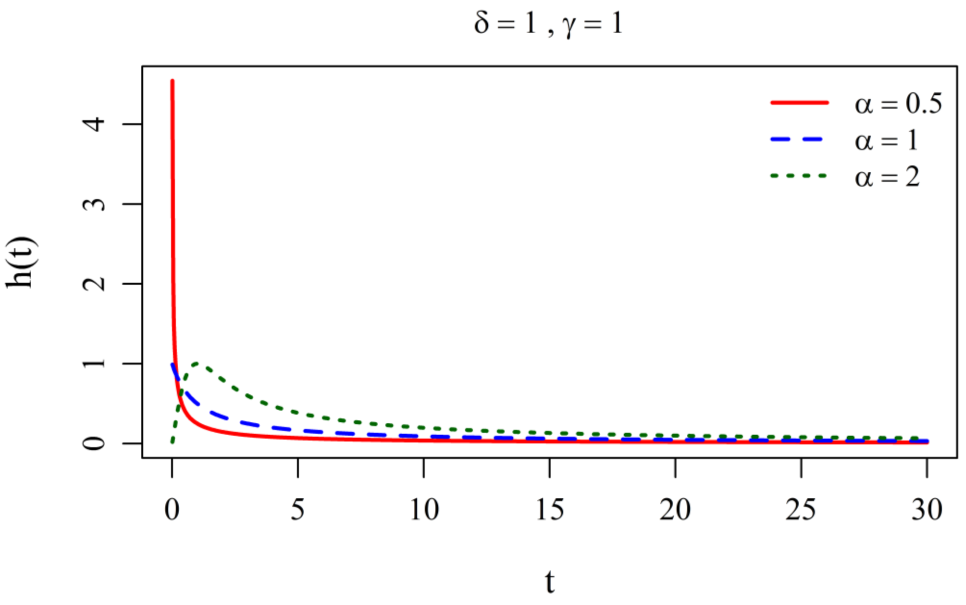

Figure 1. The hazard rate functions of the CW distribution for different values of the shape parameter α under fixed values of the parameter δ and the parameter γ.

3. Designing of the control chart using compound Weibull distribution

This section presents an attribute control chart developed specifically to monitor the number of defective items in a process. The proposed chart is constructed by CW distribution within the framework of a time-truncated life test under single sampling.

The median lifetime was adopted as the quality characteristic instead of the mean lifetime because it provides a more robust measure of the central tendency for right-skewed lifetime distributions. In positively skewed distributions, such as the CW distribution, the mean is strongly influenced by a relatively small number of exceptionally long lifetimes, whereas the median remains stable and represents the typical lifetime of a product. Moreover, the median corresponds to the 50th percentile, indicating the time by which half of the units have failed and half remain operational. Therefore, monitoring shifts in the median lifetime offers a more reliable and practically meaningful assessment of process performance under skewed lifetime distributions.

Let m_0 denote the target median lifetime when the process is in control. Suppose that the shift in the process median is to be monitored by observing the number of failed items up to a predetermined termination time t_0. A failed item is defined as an item whose lifetime is less than m_0. However, since a truncated life test is considered here, a failed item is defined as an item that fails before the specified truncation time $t_0 = am$. When, for example, m_0=800 hours and a=0.1, it means that the life test duration is just 10% of the target lifetime median.

The probability that an item fails during the truncation time t_0 is denoted by $p = F_T(t_0)$. If the process is in statistical control (i.e $m = m_0$), the probability of failure is denoted by p_0.

The probability that an item fails before the truncation time $t_0 = am_0$ for the CW distribution using Equation (2) and (4) is given by

$$p_0 = F_T(t_0) = 1 - \frac{\delta^\gamma}{((am_0)^\alpha + \delta)^\gamma}; \qquad t > 0,\ \alpha, \gamma, and\ \delta > 0 \tag{6}$$

$$m_0^\alpha = \delta(2^{\frac{1}{\gamma}} - 1)$$

$$(am_0)^\alpha = a^\alpha \delta(2^{\frac{1}{\gamma}} - 1) \tag{7}$$

By replacing the median expression in Equation (6) with Equation (7), the in-control failure probability is expressed as

$$\begin{aligned} p_0 = F_T(t_0) &= 1 - \frac{\delta^\gamma}{[a^\alpha \delta(2^{1/\gamma} - 1) + \delta]^\gamma} \\ &= 1 - \frac{\delta^\gamma}{\{\delta[1 + a^\alpha(2^{1/\gamma} - 1)]\}^\gamma} \\ &= 1 - \frac{\delta^\gamma}{\delta^\gamma[1 + a^\alpha(2^{1/\gamma} - 1)]^\gamma} \end{aligned}$$

$$p_0 = F_T(t_0) = 1 - \left[1 + a^\alpha\left(2^{1/\gamma} - 1\right)\right]^{-\gamma} \tag{8}$$

In the study, the scale parameter of the distribution under investigation is considered as the quality characteristic, while the remaining parameters in the distribution function are assumed to be known.

The steps for constructing an np control chart for the number of failed items for CW distributions are given as follows:

Step 1. *For each subgroup, a sample of size* n *is taken from the production process. The number of items that fail before the truncation time* $t_0 = am_0$ *is denoted by* D.

Step 2. *If* $D > UCL$ *or* $D < LCL$ *the process is declared out of control; otherwise, it is considered to be in control if* $LCL \leq D \leq UCL$.

The random variable D, representing the number of failed items, can be assumed to follow a binomial distribution with parameters n and p. Accordingly, the control limits of the np control chart are given by

$$\text{UCL} = np_o + k\sqrt{np_0(1-p_0)}$$

$$\text{LCL} = max\left[0, np_o - k\sqrt{np_0(1-p_0)}\right] \tag{9}$$

In Equation (9) k denotes the control chart constant.

When the failure probability p_0 is unknown, it is estimated from an initial sample collected while the process is assumed to be in control. Consequently, in the case where the standards are unknown, the control limits of the chart are given by,

$$\text{UCL} = \bar{D} + k\sqrt{\bar{D}(1-\frac{\bar{D}}{n})}$$

$$\text{LCL} = max\left[0, \bar{D} - k\sqrt{\bar{D}(1-\frac{\bar{D}}{n})}\right] \tag{10}$$

In Equation (10), $\bar{D}$ is the average of the number of failures in the subgroup through a previous sample.

The in-control ARL (ARL_0) is related to the probability of a Type I error, whereas the out-of-control ARL (ARL_1) depends on the probability of a Type II error.

When the process is in control (i.e., $m = m_0$ and possibility of failure p_0), the in-control probability of the process is given by

$$1-\alpha = P(LCL \leq D \leq UCL | p_0) = \sum_{d=\lfloor LCL \rfloor+1}^{\lceil UCL \rceil} \binom{n}{d} p_0^{\,d}(1-p_0)^{n-d} \tag{11}$$

where $\lceil \cdot \rceil$ and $\lfloor \cdot \rfloor$ denote the ceiling and floor functions, respectively. In Equation (11), when the lower control limit (LCL) is equal to zero, the value of d should be taken as zero.

Suppose that the process median shifts from m_0 to $m_1 = bm_0$, where b denotes the shift parameter. In this case, if the failure probability given in Equation (8) is denoted by p_1 for CW distribution, then,

$$p_1 = 1 - \left[1 + (\tfrac{a}{b})^\alpha (2^{1/\gamma} - 1)\right]^{-\gamma} \tag{12}$$

The in-control process median m_0 corresponds to the failure probability p_0, whereas the out-of-control process median m_1 corresponds to the failure probability p_1. When the process median shifts from m_0 to m_1, the probability that the process remains in control corresponds to the Type II error:

$$\beta = P(LCL \leq D \leq UCL/p_1) = \sum_{d=\lfloor LCL \rfloor+1}^{\lfloor UCL \rfloor} \binom{n}{d} p_1^d (1-p_1)^{n-d} \tag{13}$$

In Equation (13), when the LCL is equal to zero, the value of d should be taken as zero.

When the performance of a control chart is evaluated by;

$$ARL_0 = \frac{1}{\alpha} \text{ and } ARL_1 = \frac{1}{1-\beta} \quad (14)$$

The computations necessary for constructing the ARL table of the proposed charts based on the CW distribution under all three scenarios are carried out as follows:

(1) Determine the specified values of ARL, say r_0 , shift parameter and sample size n.

(2) Determine the values of a and k based on the specified different sample size n, ensuring that ARL_0 in Equation (14) is approaches to r_0,

(3) Using the values of a and k obtained in step 2 to compute the values of ARL_1 for different values of shifted constant.

4. Performance measures

Although the ARL is the most adopted measure for assessing the performance of statistical process monitoring schemes, relying solely on ARL may not provide a complete evaluation of a control chart. This is because ARL only reflects the expected number of samples required before an out-of-control signal is generated. To address this limitation, recent studies have advocated the use of additional performance measures that capture different aspects of a control chart's detection capability. Unlike the use of ARL alone, these measures evaluate performance across a range of process shift magnitudes while also accounting for the variability in run length, thereby providing a more comprehensive basis for comparing competing control charts [8], [3], [11]. Accordingly, the proposed attribute control chart is also assessed using three complementary performance criteria: EARL, EQL, and SDRL.

On the other hand, while the multiplicative change factor in the process mean is denoted by b, the net shift size is explicitly defined by the parameter ω. When the process is in-control (b = 1.00), the net shift size is zero (ω = 0). The net shift size representing the deviation from the target value is formulated as follows:

$$\omega_i = b_i - 1, \qquad i = 1,2, \ldots, s$$

Where s denotes the number of out-of-control shift magnitudes considered in the performance evaluation. Based on this definition, $\omega_i \rangle 0$ indicates an upward shift (an increase in the process median), whereas $\omega_i \langle 0$ indicates a downward shift (a decrease in the process median). The in-control state ($\omega_i = 0$) is excluded from the performance analysis.

The EARL is defined as the average of the out-of-control ARL values over a specified range of shift magnitudes or represents the expected number of subgroups that the control chart must inspect before generating an alarm signal when a random shift occurs in the process. Assuming that the shift magnitudes follow a discrete uniform distribution (i.e., each out-of-control shift is equally likely), the EARL is calculated as

$$EARL = \frac{\sum_{i=1}^{s} ARL(\omega_i)}{s} \quad (15)$$

EQL provides an overall performance measure by assigning greater weight to larger process shifts. It is computed as

$$EQL = \frac{1}{\omega_{max}-\omega_{min}} \int_{\omega_{min}}^{\omega_{max}} ARL(\omega) d\omega \approx \frac{1}{s} \sum_{i=1}^{s} \omega_i^2 \, ARL(\omega_i) \quad (16)$$

Smaller values of both EARL and EQL indicate better overall detection performance.

In addition to the average performance measures, the variability of the run length is evaluated by the SDRL. Since the run length follows a geometric distribution, the SDRL can be directly obtained from the corresponding ARL value as

$$SDRL_i = \sqrt{ARL(\omega_i)[ARL(\omega_i) - 1]} \tag{17}$$

The SDRL measures the dispersion of the run length around its mean. Smaller SDRL values indicate that the control chart signals process shifts more consistently, whereas larger SDRL values imply greater variability in the detection time.

5. Discussion and results

This section presents the results obtained from the analysis of the distribution of survival data. Tables 1-9 show the ARL, EARL, EQL and SDRL values for various shift parameters (b=1, 0,9, 0.8, 0.7, 0.6, 0.5, 0.4, 0.3, 0.2, 0.1). The target ARL_0 (r_0) values in this study are 200, 250, 370 while the sample sizes are 20, 30, 40 ,50 with an unknown δ scale parameter and a target median life m_0=800. The values of the truncation coefficient and the control chart constant k were determined based on target values of the ARL.

The findings can be summarized as follows:

(1) The ARL_1 value decreases as the magnitude of the process shift increases. For example, as shown in Table 1, with r_0 = 200, n = 20, and α = $2.5, \gamma = 1$, the ARL_1 value is 137.35 when b = 0.9. As the shift becomes larger (b = 0.4), the ARL_1 decreases sharply to 2.53 and equals 1.000 at b = 0.1. This pattern shows that larger process shifts are detected more rapidly.

(2) The sensitivity of the proposed control chart increases with sample size. As presented in Tables 3 and 4, for r_0 = 200 and α = $2.5, \gamma = 2$, the ARL_1 value reaches 1.0 at b = 0.2 when n = 20, whereas the same value is reached at b = 0.5 when n = 50. These results indicate that increasing the sample size allows the proposed control chart to detect process shifts at smaller shift magnitudes.

(3) It was observed that when the target value r_0 increased while the deviation parameter remained constant, the ARL_1 values also increased slightly. This is because a larger target ARL_0 implies wider control limits. Consequently, more samples are needed before the chart signals the same magnitude of process shift.

(4) As presented in Tables 1–8, the EARL, EQL, and SDRL performance measures describe different aspects of the proposed control chart performance. The SDRL values exhibit a trend similar to that of ARL_1. The highest SDRL values are observed under the in-control condition, and they decrease as the magnitude of the process shift increases. This trend indicates a reduction in the variability of the run length with increasing process shift magnitude. A similar pattern is observed for the EARL and EQL performance measures. Both EARL and EQL increase as the target in-control ARL (ARL_0) increases, reflecting the relationship between the false alarm rate and the detection of process shifts. Overall, the results show that the proposed control chart satisfies the specified in-control ARL (ARL_0) requirement over a range of process shift magnitudes.

(5) Figures 2–5 illustrate the ARL_1 profiles of the proposed attribute control chart for different combinations of the CW shape parameters (α = 2.5 and 3; γ = 1 and 2). Across all parameter settings, a consistent performance pattern is observed. The ARL_1 values remain close to one for large process shifts and increase rapidly as the shift parameter approaches the in-control state (b → 1), indicating that the proposed chart can detect substantial process deterioration with only a few samples while requiring more samples to identify smaller shifts. For every parameter combination, increasing the target in-control

performance from $ARL_0 = 200$ to $ARL_0 = 370$ results in higher ARL_1 values near the in-control region, reflecting the expected trade-off between false alarm protection and detection speed. Furthermore, increasing the sample size from 20 to 50 consistently improves the sensitivity of the proposed chart, leading to faster detection of small and moderate process shifts while maintaining similar performance for large shifts. A slight difference among the figures is observed for $\gamma = 2$, where the ARL_1 curves rise more steeply as b approaches one than in the corresponding $\gamma = 1$ cases. This suggests that increasing the shape parameter γ has a more pronounced effect on the detection performance when the process shift is relatively small, whereas the overall monitoring behavior remains largely unchanged across the considered parameter settings.

Table 1. ARL_1 values under the CW distribution ($\alpha = 2.5;\ \gamma = 1$) n = 20, 30

	n = 20						**n = 30**					
	$r_0 = 200$		**$r_0 = 250$**		**$r_0 = 370$**		**$r_0 = 200$**		**$r_0 = 250$**		**$r_0 = 370$**	
LCL	**2.74**		**1.17**		**1.98**		**0.43**		**2.94**		**4.45**	
UCL	**14.02**		**13.59**		**14.53**		**13.71**		**17.65**		**20.96**	
a	**0.76**		**0.63**		**0.74**		**0.36**		**0.57**		**0.77**	
k	**2.56**		**2.88**		**2.85**		**2.86**		**2.83**		**3.05**	
b	**ARL_1**	**SDRL**	**ARL_1**	**SDRL**	**ARL_1**	**SDRL**	**ARL_1**	**SDRL**	**ARL_1**	**SDRL**	**ARL_1**	**SDRL**
1	**200**	199.49	**249.99**	249.49	**369.95**	369.45	**200**	199.5	**250.01**	249.51	**369.95**	369.45
0.9	137.35	136.85	150.61	150.11	181.93	181.43	93.85	93.35	109.69	109.19	170.1	169.6
0.8	66.75	66.25	70.88	70.37	79.31	78.81	41.28	40.78	43.58	43.08	62.72	62.22
0.7	28.96	28.46	30.71	30.21	33.26	32.76	17.76	17.25	17.14	16.63	22.64	22.13
0.6	12.32	11.81	13.05	12.54	13.84	13.33	7.68	7.17	6.96	6.44	8.48	7.96
0.5	5.37	4.85	5.64	5.12	5.89	5.36	3.48	2.94	3.07	2.52	3.49	2.94
0.4	2.53	1.97	2.62	2.06	2.7	2.14	1.78	1.18	1.6	0.98	1.72	1.11
0.3	1.41	0.77	1.43	0.79	1.46	0.82	1.15	0.42	1.1	0.33	1.13	0.38
0.2	1.05	0.23	1.05	0.23	1.06	0.24	1.01	0.07	1	0.05	1	0.07
0.1	1	0.01	1	0.01	1	0.02	1	0	1	0	1	0
EARL	**28.53**		**30.78**		**35.61**		**18.78**		**20.57**		**30.25**	
EQL	**1.45**		**1.53**		**1.65**		**0.99**		**0.98**		**1.23**	

Table 2. ARL_1 values under the CW distribution ($\alpha = 2.5$; $\gamma = 1$) n = 40, 50

	n = 40						n = 50					
	r_0 = 200		r_0 = 250		r_0 = 370		r_0 = 200		r_0 = 250		r_0 = 370	
LCL	**6.77**		**4.45**		**4.89**		**9.42**		**7.1**		**12.91**	
UCL	**23.37**		**21.85**		**22.61**		**28.31**		**26.68**		**33.72**	
a	**0.65**		**0.54**		**0.57**		**0.65**		**0.56**		**0.89**	
k	**2.71**		**2.93**		**2.95**		**2.76**		**2.93**		**2.95**	
b	**ARL_1**	**SDRL**	**ARL_1**	**SDRL**	**ARL_1**	**SDRL**	**ARL_1**	**SDRL**	**ARL_1**	**SDRL**	**ARL_1**	**SDRL**
1	**199.98**	199.48	**250**	249.5	**369.98**	369.48	200	199.5	249.97	249.47	369.97	369.47
0.9	94.03	93.53	105.44	104.94	141.96	141.46	97.02	96.52	111.33	110.83	138.39	137.89
0.8	33.52	33.01	37.61	37.11	47.7	47.2	30.98	30.48	35.48	34.97	39.03	38.53
0.7	11.97	11.46	13.5	12.99	16.22	15.72	10.1	9.59	11.52	11.01	11.72	11.21
0.6	4.65	4.12	5.19	4.67	5.92	5.4	3.76	3.22	4.2	3.67	4.09	3.56
0.5	2.12	1.54	2.31	1.74	2.5	1.93	1.75	1.15	1.89	1.3	1.83	1.23
0.4	1.26	0.57	1.31	0.64	1.36	0.7	1.14	0.39	1.17	0.44	1.15	0.42
0.3	1.02	0.15	1.03	0.18	1.04	0.2	1.01	0.08	1.01	0.1	1.01	0.09
0.2	1	0.01	1	0.01	1	0.02	1	0	1	0	1	0
0.1	1	0	1	0	1	0	1	0	1	0	1	0
EARL	**16.73**		**18.71**		**24.3**		**16.42**		**18.73**		**22.13**	
EQL	**0.78**		**0.85**		**0.98**		**0.72**		**0.79**		**0.83**	

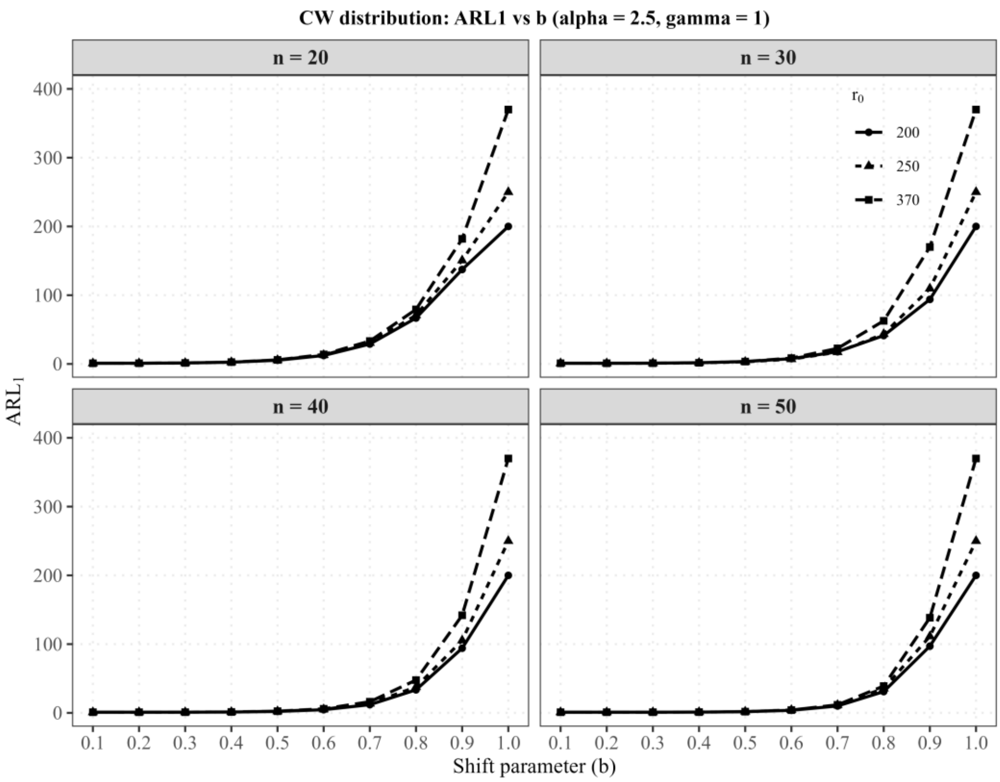

Figure 2. ARL_1 curves for the CW distribution with $\alpha = 2.5$ and $\gamma = 1$ under different sample sizes (n = 20, 30, 40, and 50) for target in-control ARL values of 200, 250, and 370.

Table 3. ARL_1 values under the CW distribution ($\alpha = 2.5;\ \gamma = 2$) n = 20, 30

	n = 20						n = 30					
	r_0 = 200		r_0 = 250		r_0 = 370		r_0 = 200		r_0 = 250		r_0 = 370	
LCL	**5.76**		**4**		**0.88**		**4.85**		**2.81**		**5.79**	
UCL	**17.48**		**17.08**		**13.82**		**19.7**		**17.78**		**21.32**	
a	**1.14**		**1.05**		**0.79**		**0.86**		**0.76**		**0.92**	
k	**2.66**		**2.93**		**3**		**2.76**		**2.88**		**2.85**	
b	**ARL_1**	**SDRL**	**ARL_1**	**SDRL**	**ARL_1**	**SDRL**	**ARL_1**	**SDRL**	**ARL_1**	**SDRL**	**ARL_1**	**SDRL**
1	**200.01**	199.51	**294.34**	293.84	**369.87**	369.37	**200.03**	199.53	**250.06**	249.56	**369.96**	369.46
0.9	88.96	88.46	300.02	299.52	81.6	81.1	41.77	41.26	47.87	47.36	79.84	79.34
0.8	21.29	20.79	61.28	60.78	19.05	18.54	8.65	8.13	9.91	9.4	13.75	13.24
0.7	6.11	5.59	13.25	12.74	5.33	4.81	2.58	2.02	2.85	2.3	3.42	2.88
0.6	2.37	1.8	3.83	3.29	2.03	1.45	1.27	0.59	1.33	0.66	1.44	0.79
0.5	1.33	0.66	1.65	1.04	1.18	0.46	1.02	0.14	1.02	0.16	1.04	0.2
0.4	1.05	0.22	1.11	0.34	1.01	0.1	1	0.01	1	0.01	1	0.02
0.3	1	0.05	1.01	0.08	1	0.01	1	0	1	0	1	0
0.2	1	0	1	0.01	1	0	1	0	1	0	1	0
0.1	1	0	1	0	1	0	1	0	1	0	1	0
EARL	**13.79**		**42.68**		**12.58**		**6.59**		**7.44**		**11.5**	
EQL	**0.591**		**1.11**		**0.55**		**0.42**		**0.43**		**0.49**	

Table 4. ARL_1 values under the CW distribution ($\alpha = 2.5;\ \gamma = 2$) n = 40, 50

	n = 40						n = 50					
	r_0 = 200		r_0 = 250		r_0 = 370		r_0 = 200		r_0 = 250		r_0 = 370	
LCL	**6.31**		**10.84**		**4.89**		**12.87**		**12.72**		**0.78**	
UCL	**23.83**		**28.73**		**22.61**		**33**		**32.26**		**16.16**	
a	**0.81**		**0.99**		**0.76**		**0.93**		**0.92**		**0.49**	
k	**2.86**		**2.83**		**2.95**		**2.86**		**2.78**		**2.9**	
b	**ARL_1**	**SDRL**	**ARL_1**	**SDRL**	**ARL_1**	**SDRL**	**ARL1**	**SDRL**	**ARL1**	**SDRL**	**ARL1**	**SDRL**
1	**200**	199.5	**250.01**	249.51	**369.96**	369.46	**223.94**	223.44	**250**	249.5	**370.02**	369.52
0.9	37.24	36.73	42.45	41.95	53.22	52.72	29.28	28.77	39.27	38.77	59.43	58.93
0.8	6.69	6.17	7	6.48	8.75	8.23	4.7	4.17	5.67	5.15	11.01	10.5
0.7	1.99	1.4	2.02	1.43	2.32	1.75	1.53	0.9	1.66	1.05	2.86	2.31
0.6	1.12	0.36	1.13	0.38	1.17	0.45	1.04	0.2	1.05	0.23	1.28	0.59
0.5	1	0.05	1	0.06	1.01	0.07	1	0.02	1	0.02	1.01	0.11
0.4	1	0	1	0	1	0	1	0	1	0	1	0
0.3	1	0	1	0	1	0	1	0	1	0	1	0
0.2	1	0	1	0	1	0	1	0	1	0	1	0
0.1	1	0	1	0	1	0	1	0	1	0	1	0
EARL	**5.78**		**6.4**		**7.83**		**4.62**		**5.85**		**8.84**	
EQL	**0.39**		**0.4**		**0.43**		**0.37**		**0.39**		**0.45**	

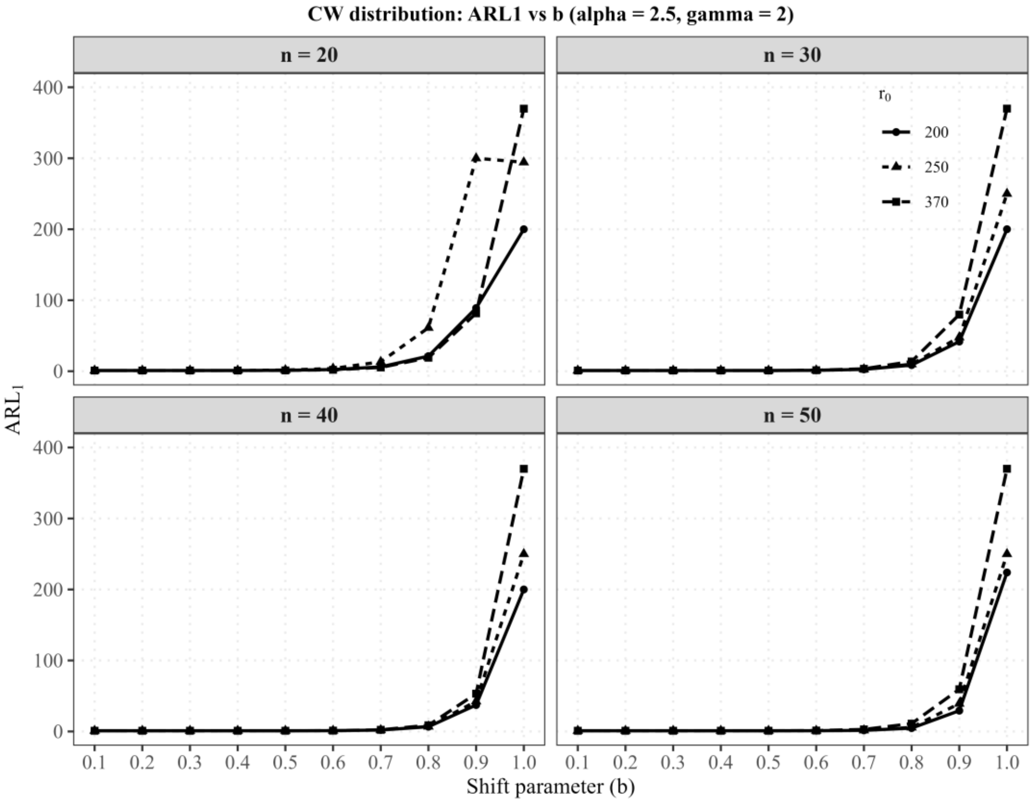

Figure 3. ARL₁ curves for the CW distribution with α = 2.5 and γ = 2 under different sample sizes (n = 20, 30, 40, and 50) for target in-control ARL values of 200, 250, and 370.

Table 5. ARL_1 values under the CW distribution ($\alpha = 3;\ \gamma = 1$) n=20, 30

	n = 20						**n = 30**					
	r_0 = 200		**r_0 = 250**		**r_0 = 370**		**r_0 = 200**		**r_0 = 250**		**r_0 = 370**	
LCL	**0.78**		**1.39**		**1.65**		**0.2**		**3.36**		**2.62**	
UCL	**12.9**		**13.38**		**14.86**		**13.95**		**18.84**		**17**	
a	**0.58**		**0.64**		**0.75**		**0.36**		**0.64**		**0.54**	
k	**2.86**		**2.78**		**3**		**2.96**		**2.93**		**2.8**	
b	**ARL_1**	**SDRL**	**ARL_1**	**SDRL**	**ARL_1**	**SDRL**	**ARL_1**	**SDRL**	**ARL_1**	**SDRL**	**ARL_1**	**SDRL**
1	**199.99**	199.49	**249.99**	249.49	**370**	369.5	**199.93**	199.43	**250.01**	249.51	**364.54**	364.04
0.9	97.9	97.4	149.1	148.6	179.5	179	93.16	92.66	119.2	118.7	183.22	182.72
0.8	45.36	44.86	69.19	68.69	77.04	76.54	40.66	40.16	46.25	45.75	70.3	69.8
0.7	20.5	19.99	29.58	29.07	31.82	31.32	17.36	16.86	17.51	17	25.62	25.11
0.6	9.22	8.71	12.42	11.91	13.06	12.55	7.47	6.95	6.87	6.35	9.49	8.98
0.5	4.26	3.72	5.32	4.8	5.5	4.98	3.37	2.83	2.97	2.42	3.79	3.25
0.4	2.13	1.56	2.47	1.9	2.52	1.96	1.73	1.13	1.55	0.92	1.78	1.18
0.3	1.28	0.6	1.37	0.71	1.39	0.74	1.13	0.39	1.08	0.3	1.13	0.39
0.2	1.02	0.15	1.04	0.19	1.04	0.2	1	0.06	1	0.04	1	0.06
0.1	1	0	1	0.01	1	0.01	1	0	1	0	1	0
EARL	**20.3**		**30.16**		**34.76**		**18.54**		**21.94**		**33.04**	
EQL	**1.12**		**1.47**		**1.59**		**0.98**		**1**		**1.34**	

Table 6. ARL_1 values under the CW distribution ($\alpha = 3$; $\gamma = 1$) n = 40, 50

	n = 40						n = 50					
	r_0 = 200		r_0 = 250		r_0 = 370		r_0 = 200		r_0 = 250		r_0 = 370	
LCL	**3.252**		**4.451**		**4.887**		**9.586**		**9.98**		**11.824**	
UCL	**19.934**		**21.851**		**22.607**		**28.143**		**29.911**		**32.917**	
a	**0.465**		**0.547**		**0.58**		**0.658**		**0.711**		**0.841**	
k	**2.907**		**2.928**		**2.95**		**2.707**		**2.878**		**3**	
b	**ARL_1**	**SDRL**	**ARL_1**	**SDRL**	**ARL_1**	**SDRL**	**ARL_1**	**SDRL**	**ARL_1**	**SDRL**	**ARL_1**	**SDRL**
1	**199.97**	199.47	**250.03**	249.53	**370.03**	369.52	**200.01**	199.51	**250.04**	249.54	**370.04**	369.54
0.9	87.4	86.9	104.1	103.6	139.92	139.42	95.48	94.98	88.44	87.94	129.34	128.84
0.8	32.71	32.21	36.62	36.12	46.31	45.8	29.92	29.41	26.85	26.35	35.99	35.49
0.7	12.24	11.73	12.99	12.48	15.55	15.04	9.63	9.12	8.73	8.22	10.75	10.24
0.6	4.88	4.35	4.96	4.44	5.63	5.1	3.57	3.02	3.31	2.76	3.77	3.23
0.5	2.22	1.65	2.21	1.63	2.38	1.81	1.68	1.07	1.61	0.99	1.71	1.1
0.4	1.29	0.61	1.28	0.59	1.31	0.64	1.11	0.35	1.1	0.33	1.12	0.36
0.3	1.03	0.17	1.02	0.16	1.03	0.17	1	0.06	1	0.06	1	0.07
0.2	1	0.01	1	0.01	1	0.01	1	0	1	0	1	0
0.1	1	0	1	0	1	0	1	0	1	0	1	0
EARL	**15.97**		**18.35**		**23.79**		**16.04**		**14.78**		**20.63**	
EQL	**0.78**		**0.83**		**0.95**		**0.71**		**0.67**		**0.79**	

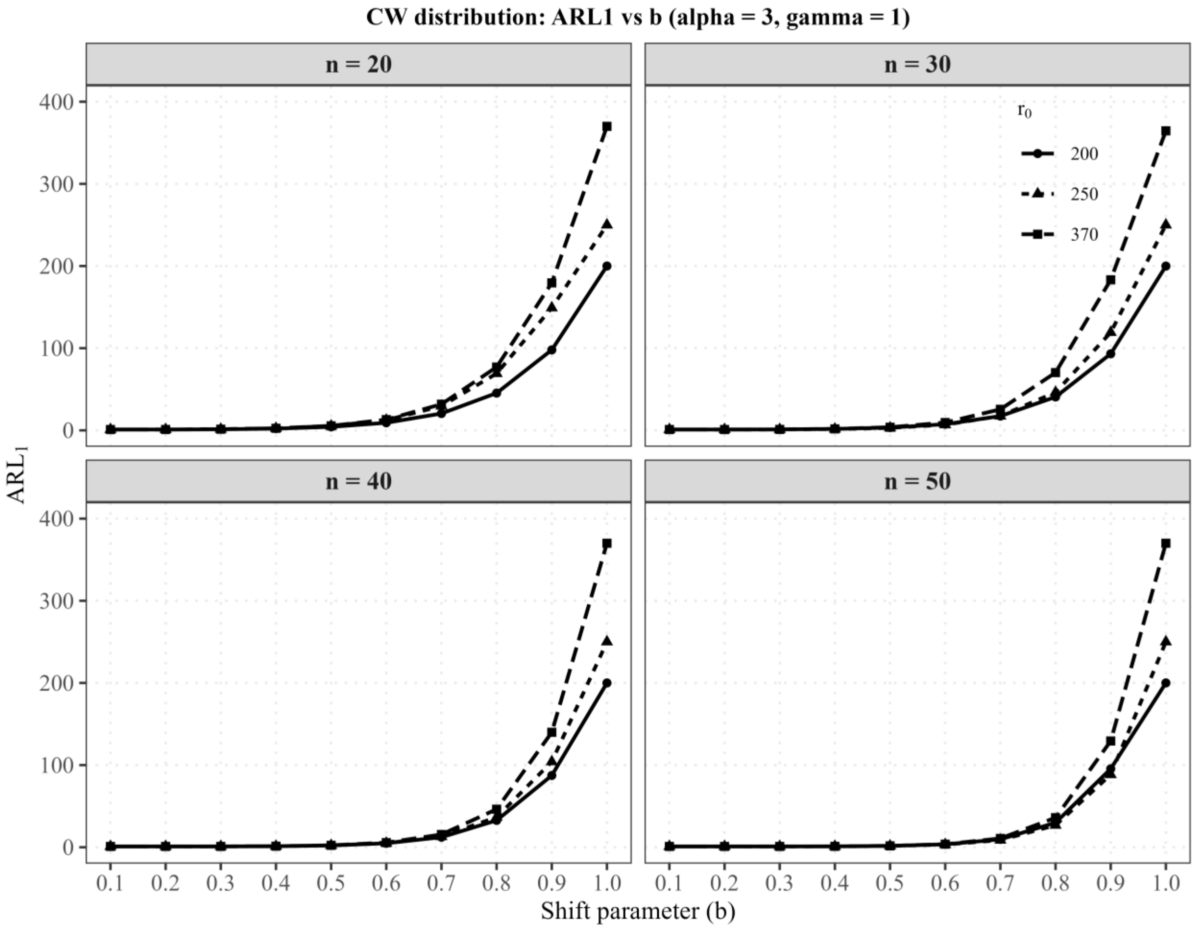

Figure 4. ARL_1 curves for the CW distribution with α = 2.5 and γ = 2 under different sample sizes (n = 20, 30, 40, and 50) for target in-control ARL values of 200, 250, and 370.

Table 7. ARL_1 values under the CW distribution ($\alpha = 3;\ \gamma = 2$) n = 20, 30

	n = 20						**n = 30**					
	r_0 = 200		**r_0 = 250**		**r_0 = 370**		**r_0 = 200**		**r_0 = 250**		**r_0 = 370**	
LCL	**5.76**		**4**		**2.83**		**1.62**		**2.81**		**2.9**	
UCL	**17.48**		**17.08**		**15.54**		**15.83**		**17.79**		**18.98**	
a	**1.14**		**1.04**		**0.94**		**0.68**		**0.76**		**0.79**	
k	**2.66**		**2.93**		**2.85**		**2.86**		**2.88**		**3.05**	
b	**ARL_1**	**SDRL**	**ARL_1**	**SDRL**	**ARL_1**	**SDRL**	**ARL_1**	**SDRL**	**ARL_1**	**SDRL**	**ARL_1**	**SDRL**
1	**200.01**	199.51	**294.39**	293.89	**369.95**	369.45	**200.03**	199.53	**249.84**	249.34	**370.01**	369.5
0.9	85.4	84.9	290.41	289.91	94.03	93.53	41.12	40.62	46.68	46.18	60.37	59.86
0.8	19.63	19.13	56.29	55.79	20.24	19.73	9.14	8.63	9.49	8.97	11.23	10.71
0.7	5.52	5	11.83	11.32	5.37	4.85	2.74	2.19	2.71	2.16	2.97	2.42
0.6	2.15	1.58	3.41	2.86	2.01	1.42	1.31	0.63	1.29	0.61	1.33	0.66
0.5	1.25	0.56	1.52	0.88	1.18	0.45	1.02	0.14	1.02	0.13	1.02	0.15
0.4	1.03	0.17	1.07	0.27	1.01	0.1	1	0	1	0	1	0
0.3	1	0.03	1	0.05	1	0	1	0	1	0	1	0
0.2	1	0	1	0	1	0	1	0	1	0	1	0
0.1	1	0	1	0	1	0	1	0	1	0	1	0
EARL	**13.11**		**40.84**		**14.09**		**6.59**		**7.24**		**8.99**	
EQL	**0.567**		**1.05**		**0.57**		**0.42**		**0.43**		**0.45**	

Table 8. ARL_1 values under the CW distribution ($\alpha = 3;\ \gamma = 2$) n = 40, 50

	n = 40						**n = 50**					
	r_0 = 200		**r_0 = 250**		**r_0 = 370**		**r_0 = 200**		**r_0 = 250**		**r_0 = 370**	
LCL	**6.62**		**9.71**		**0.88**		**25.81**		**12.72**		**14.71**	
UCL	**23.52**		**27.88**		**16.55**		**43.75**		**32.26**		**35.92**	
a	**0.81**		**0.95**		**0.57**		**1.37**		**0.92**		**1.01**	
k	**2.76**		**2.88**		**3**		**2.76**		**2.78**		**3**	
b	**ARL_1**	**SDRL**	**ARL_1**	**SDRL**	**ARL_1**	**SDRL**	**ARL_1**	**SDRL**	**ARL_1**	**SDRL**	**ARL_1**	**SDRL**
1	**200.01**	199.51	**249.96**	249.46	**369.79**	369.28	**200.01**	199.51	**249.99**	249.49	**369.98**	369.48
0.9	36.13	35.62	39.43	38.93	59.33	58.83	41.01	40.5	37.56	37.06	43.5	43
0.8	6.36	5.84	6.42	5.9	11.13	10.62	6.07	5.55	5.3	4.78	5.72	5.2
0.7	1.9	1.3	1.88	1.28	2.91	2.36	1.81	1.21	1.58	0.95	1.63	1.01
0.6	1.1	0.33	1.09	0.32	1.29	0.62	1.1	0.32	1.04	0.2	1.04	0.22
0.5	1	0.04	1	0.04	1.01	0.12	1	0.06	1	0.01	1	0.02
0.4	1	0	1	0	1	0	1	0	1	0	1	0
0.3	1	0	1	0	1	0	1	0	1	0	1	0
0.2	1	0	1	0	1	0	1	0	1	0	1	0
0.1	1	0	1	0	1	0	1	0	1	0	1	0
EARL	**5.61**		**5.98**		**8.85**		**6.11**		**5.61**		**6.32**	
EQL	**0.39**		**0.39**		**0.45**		**0.39**		**0.38**		**0.39**	

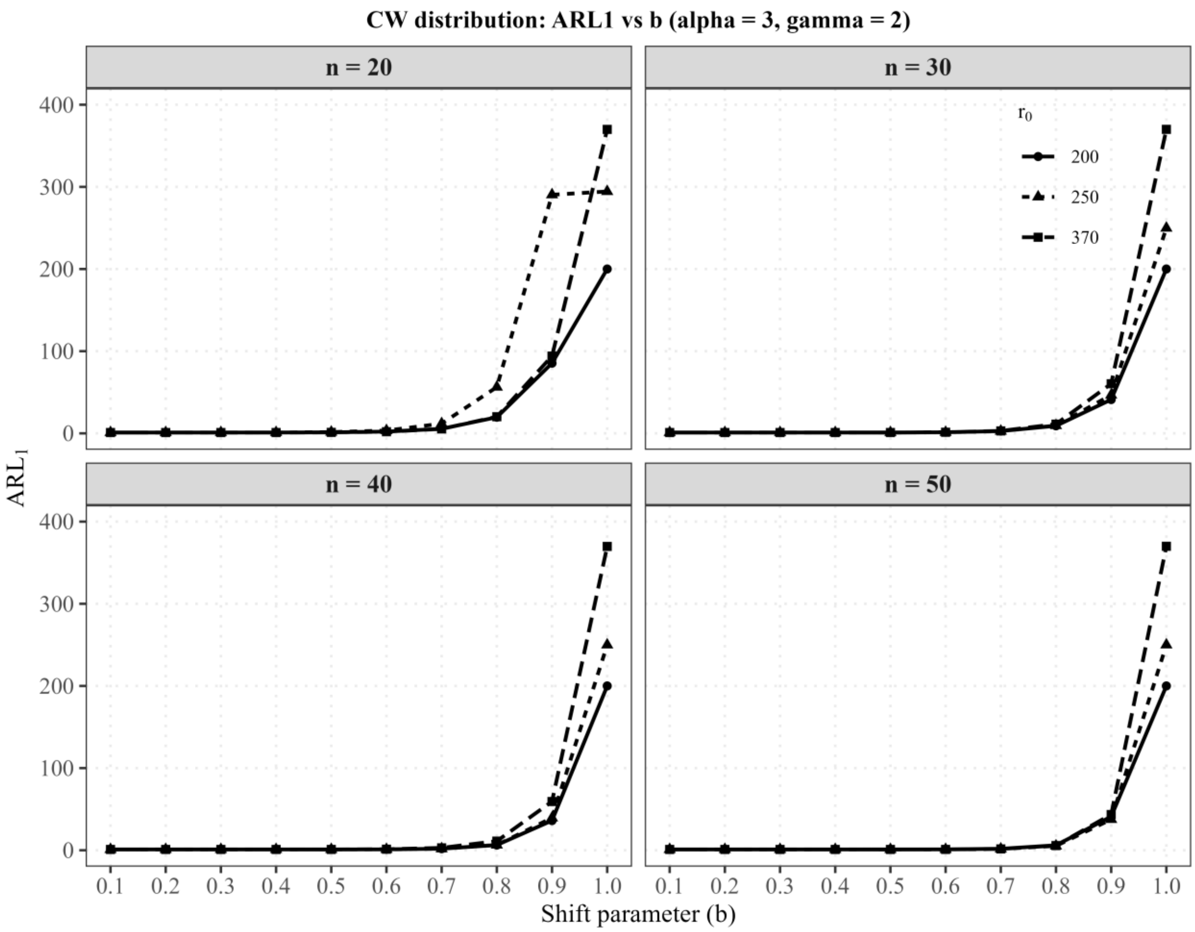

Figure 5. ARL_1 curves for the CW distribution with α = 3 and γ = 2 under different sample sizes (n = 20, 30, 40, and 50) for target in-control ARL values of 200, 250, and 370.

5.1. Performance comparison of the CW, Weibull and Exponential control charts

A comparative performance analysis of the attribute np control charts based on the CW, Weibull, and Exponential distributions was conducted. For this purpose, the control charts were evaluated under sample sizes of $n = 30$, 40, and 50, and target in-control average run lengths of $r_0 = 200, 250$ and 370. The out-of-control performance was examined for different values of the shift parameter b. Representative comparison tables are presented to illustrate the relative performance of the three distribution-based control charts under various process conditions.

Table 9. Performance comparison of the CW (α = 2.5, γ = 2), Weibull ($\beta^* = 2$) and Exponential (n = 40, r_0 = 200)

	Weibull		**Exponential**		**CW**	
b	**ARL₁**	**SDRL**	**ARL₁**	**SDRL**	**ARL₁**	**SDRL**
0.1	1	0	1	0	1	0
0.2	1	0	1	0	1	0
0.3	1	0	1.00	0.04	1	0
0.4	1	0	1.08	0.30	1	0.00
0.5	1.00	0.04	1.60	0.98	1.00	0.05
0.6	1.11	0.35	3.37	2.82	1.12	0.36
0.7	2.03	1.44	9.01	8.49	1.99	1.40
0.8	6.82	6.30	27.37	26.87	6.69	6.17
0.9	34.48	33.97	85.46	84.96	37.24	36.73
1	**200.04**	**199.54**	**199.99**	**199.49**	**200.00**	**199.50**

Table 10. Performance comparison of the CW (α = 2.5, γ = 2), Weibull ($\beta^* = 2$) and Exponential (n = 40, r_0 = 370)

	Weibull		**Exponential**		**CW**	
b	**ARL₁**	**SDRL**	**ARL₁**	**SDRL**	**ARL₁**	**SDRL**
0.1	1	0	1	0	1	0
0.2	1	0	1	0.01	1	0
0.3	1	0	1.02	0.16	1	0
0.4	1	0	1.34	0.67	1	0.00
0.5	1	0.01	2.55	1.98	1.01	0.07
0.6	1.05	0.24	6.24	5.72	1.17	0.45
0.7	1.79	1.19	17.28	16.77	2.32	1.75
0.8	6.62	6.10	49.93	49.42	8.75	8.23
0.9	43.71	43.21	142.98	142.48	53.22	52.72
1	**369.86**	**369.36**	**369.85**	**369.35**	**369.96**	**369.46**

Table 11. Performance comparison of the CW (α = 2.5, γ = 2), Weibull ($\beta^* = 2$) and Exponential (n = 50, r_0 = 200)

	Weibull		**Exponential**		**CW**	
b	**ARL₁**	**SDRL**	**ARL₁**	**SDRL**	**ARL₁**	**SDRL**
0.1	1	0	1	0	1	0
0.2	1	0	1	0	1	0
0.3	1	0	1	0.01	1	0
0.4	1	0	1.03	0.18	1	0
0.5	1.00	0.02	1.37	0.71	1	0.02
0.6	1.08	0.29	2.72	2.16	1.04	0.20
0.7	1.86	1.26	7.46	6.94	1.53	0.90
0.8	6.11	5.59	24.77	24.27	4.70	4.17
0.9	31.68	31.17	87.31	86.81	29.28	28.77
1	**200.06**	**199.56**	**199.99**	**199.49**	**223.94**	**223.44**

Table 12. Performance comparison of the CW (α = 2.5, γ = 2), Weibull ($\beta^* = 2$) and Exponential (n = 50, r_0 = 370)

	Weibull		**Exponential**		**CW**	
b	**ARL₁**	**SDRL**	**ARL₁**	**SDRL**	**ARL₁**	**SDRL**
0.1	1	0	1	0	1	0
0.2	1	0	1	0	1	0
0.3	1	0	1	0.01	1	0
0.4	1	0	1.02	0.14	1	0.00
0.5	1	0	1.28	0.60	1.012	0.11
0.6	1.00	0.05	2.52	1.96	1.28	0.59
0.7	1.23	0.53	7.40	6.88	2.86	2.31
0.8	3.73	3.19	28.06	27.55	11.01	10.50
0.9	32.34	31.84	120.69	120.19	59.43	58.93
1	**369.98**	**369.48**	**370.01**	**369.51**	**370.02**	**369.52**

As presented in Tables 9-12, the proposed chart based on the CW distribution exhibits a performance comparable to those based on the Weibull and Exponential distributions for most combinations of sample size and shift magnitude. However, at the process shift level of $b = 0.9$, the proposed control chart based on the CW distribution yields lower ARL_1 values. This result indicates that, under the assumption that product lifetimes follow the CW distribution, the lower ARL_1 values enable the proposed control chart to identify an out-of-control process within a short run length. Therefore, when product lifetime data are adequately described by the CW distribution, the proposed attribute npcontrol chart can serve as an effective tool for monitoring process shifts.

5.2. An illustrative example

Assume that the product lifetimes follow a CW distribution with a median of 800 hours, for fixed α = 2.5 and $\gamma = 1$ and unknown scale parameter. Considering a sample size of 20 in each group and an in-control ARL value of r_0 = 370, we obtain a= 0.74, k=2.85, LCL = 1.98 and UCL = 14.53 from Table 1. The functioning of the resulting control chart is as follows:

Step 1: Draw a sample of 20 products from each subgroup and test their lifetimes over a period of 0.74*800=592 hours. Based on the test results, determine the number of product failures (D).

Step 2: If 1.98 ≤ D ≤ 14.53, it indicates that the process is under control; otherwise, it indicates that it is not.

5.3. Illustrative example using simulated data

To demonstrate the practical performance of the proposed control chart, two simulated datasets corresponding to different process shift magnitudes are generated from the CW distribution using Monte Carlo simulation. The simulations are performed using R version 4.5.0 [33]. The simulation is carried out using α = 2.5 and γ = 1, while the shift parameter is taken as b = 0.7 and b = 0.3 to represent moderate and large process shifts, respectively. The resulting control charts provide an illustrative comparison of the chart's detection capability under different levels of process deterioration.

In the first illustrative study, the practical performance of the proposed control chart is illustrated under a moderate process shift ($b = 0.7$). A total of 40 subgroups, each consisting of $n = 40$observations, are generated. The first 15 subgroups are produced under the in-control condition with a target median lifetime of $m_0 = 800$, whereas the remaining 15 subgroups are generated after introducing a process shift of $b = 0.7$. The control chart is designed for a target in-control Average Run Length of $ARL_0 = 370$. Accordingly, the chart constant is selected as $k = 2.95$ from Table 2, and the termination time is determined as $t_0 = am_0 = 0.57 \times 800 = 456$. The number of failed products before the termination time, denoted by D, is calculated for each subgroup and summarized in Table 11. The average number of failures is $\bar{D} = 15.33$, while the control limits obtained from Eq. (10) are $UCL = 24.4$ and $LCL = 6.26$. The resulting control chart is presented in Figure 6(a). As shown in the figure, the proposed chart first signals an out-of-control condition at the 20th subgroup, indicating its ability to detect a moderate process shift within a relatively short monitoring period.

In the second illustrative study, the first 15 subgroups are generated under the in-control condition with a target median lifetime of $m_0 = 800$, whereas the remaining 15 subgroups are generated after introducing a large process shift ($b = 0.3$). The control chart is designed for a target in-control Average Run Length of $ARL_0 = 370$. Accordingly, the chart constant is selected as $k = 2.95$ from Table 2, and the termination time is determined as $t_0 = am_0 = 0.57 \times 800 = 456$. The number of failed products before the termination time, denoted by D, is calculated for each subgroup and summarized in Table 11. The average number of failures is $\bar{D} = 20.4$, while the control limits obtained from Eq. (10) are $UCL = 29.73$ $LCL = 11.07$. The resulting control chart is presented in Figure 6(b). As shown in the figure, the proposed chart first signals an out-of-control condition at the first out-of-control subgroup, demonstrating its ability to detect a large process shift almost immediately after the process deterioration occurs.

6. Conclusion

In this study, an attribute np control chart was developed for use under a time-truncated life test assuming that product lifetimes follow the CW distribution. The design parameters of the proposed control chart were determined for different sample sizes, shape parameter values, and target in-control ARL_0 levels. The out-of-control performance of the chart was evaluated using the ARL_1, SDRL, EARL, and EQL performance measures. The results indicate that increasing the sample size improves the performance of the proposed control chart. In particular, larger sample sizes enable the chart to detect process shifts with lower ARL_1 values, accompanied by corresponding improvements in the SDRL, EARL, and EQL measures.

To illustrate the practical implementation of the proposed control chart, an illustrative example was carried out using data generated from the CW distribution. The results demonstrate that the proposed control chart is capable of monitoring process changes and support the theoretical findings through an illustrative application.

The theoretical and illustrative results obtained in this study demonstrate the applicability of the proposed attribute np control chart to processes in which product lifetimes follow the CW distribution. Therefore, for reliability applications where product lifetime data can be adequately modeled by the CW distribution under time-truncated life tests, the proposed control chart provides a practical tool for monitoring process performance and detecting process shifts.

In conclusion, this study extends the application of attribute control charts for time-truncated life tests to the Compound Weibull distribution and provides a detailed investigation of the design and performance of the proposed control chart under this lifetime model. Future research may extend the proposed approach to other lifetime distributions, alternative sampling schemes (such as repetitive sampling and multiple deSpendent state sampling), and different process monitoring methodologies.

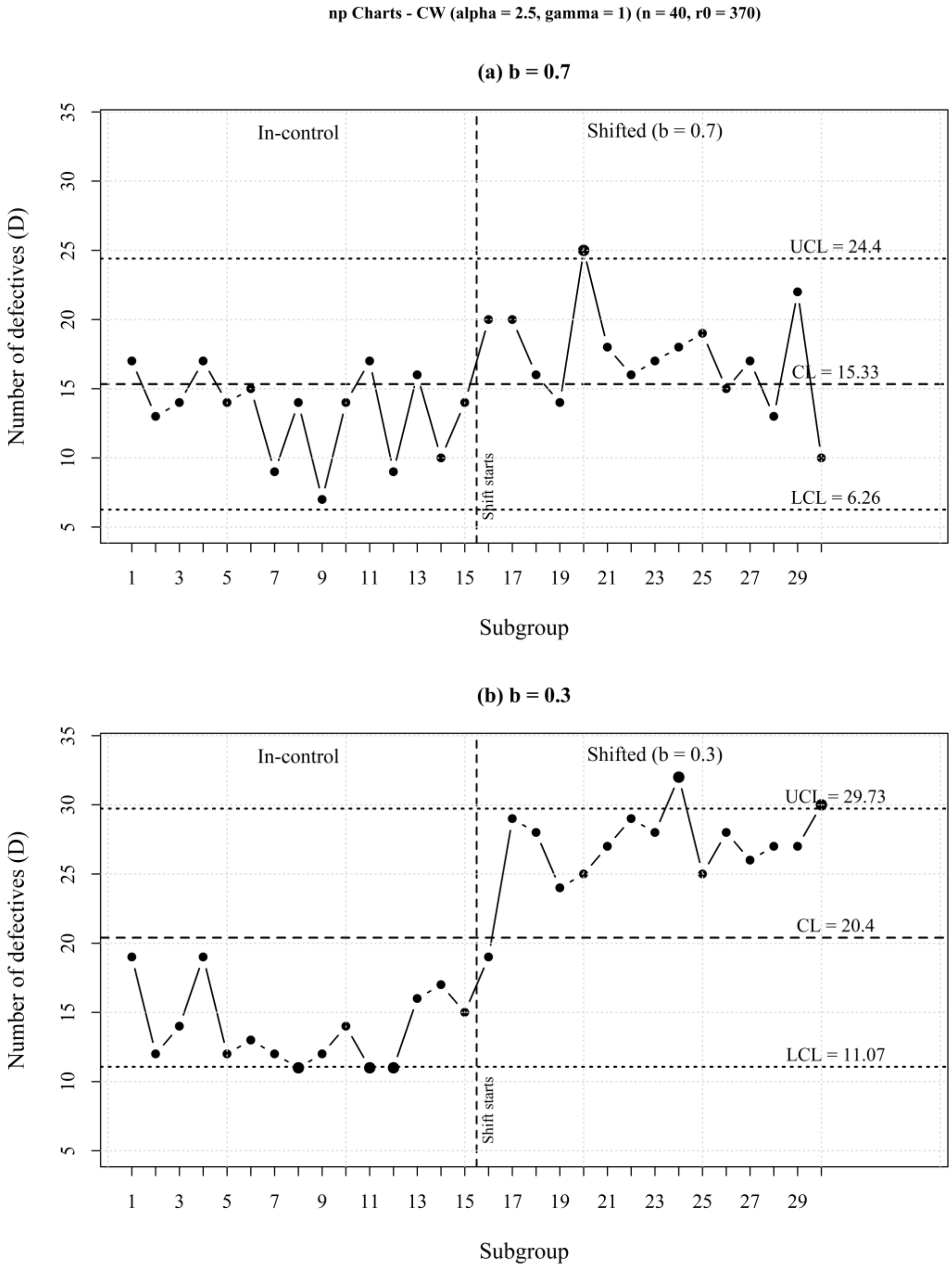

Figure 6. CW attribute control chart illustrating the detection of process shifts with different magnitudes (b = 0.7 and b = 0.3)

References

[1] D. C. Montgomery, 2009, *Introduction to Statistical Quality Control*, (6th ed) ed. New York: John Wiley & Sons, Inc; 2009.

[2] A. Shafqat et al., 2018, Attribute control chart for some popular distributions, Communications in Statistics-Theory and Methods, 47(8), 1978-1988. doi: 10.1080/03610926.2017.1335414

[3] O. A. Adeoti, G. S. Rao, M. Ahsan, 2022, Attribute control chart for Rayleigh distribution using repetitive sampling under truncated life test, Journal of Probability and Statistics, 2022(1). doi: 10.1155/2022/8763091

[4] T. Kavitha, M. Gunasekaran, 2025, Designing an attribute control chart based on exponential-Rayleigh distribution under hybrid censoring, Reliability: Theory & Applications, 20(2 (84))), 824–833. doi: 10.1080/03610918.2025.2458570

[5] N. S. Kolli, G. S. Rao, K. Rosaiah, 2025, A time truncated attribute control chart to monitor urgent physiological investigations turnaround times. Scientific Reports, 15(1), 7556. doi: 10.1038/s41598-024-78106-x

[6] C. Nanthakumar, T. Kavitha, 2017, Design of attribute control chart based on Inverse Rayleigh distribution under type-i censoring, International Journal of Scientific Research in Mathematical and Statistical Sciences, 4(6), 17-22. doi:10.26438/ijsrmss/v4i6.1722

[7] M. Saha et al., 2023, Time truncated attribute control chart for the Rayleigh distribution quality characteristics and beyond, International Journal of Quality & Reliability Management, 41(8). doi:10.1108/IJQRM-02-2023-0049

[8] E. M. Abd Elrazik, 2020, Attribute control charts for the new Weibull Pareto distribution under truncated life tests. Journal of Statistics Applications & Probability, 9(1), 43–49. doi: 10.18576/jsap/090105

[9] A. H. Al-Marshadi et al., Performance of a new time-truncated control xhart for Weibull distribution under uncertainty, 2021, International Journal of Computational Intelligence Systems, 14(1), 1256-1262. doi: 10.2991/ijcis.d.210331.00

[10] M. Aslam, O. H. Arif, C. H. Jun, An attribute control chart for a Weibull distribution under accelerated hybrid censoring, PLoS ONE, 12, e0173406.

[11] M. Aslam, C. H. Jun, 2015, Attribute control charts for the Weibull distribution under truncated life tests, Qual Eng., 27 (3), 283–288. doi:10.1080/08982112.2015.1017649

[12] A. Baklizi, S. A. Ghannam, 2022, An attribute control chart for the inverse Weibull distribution under truncated life tests, Heliyon, 8, 12. doi: 10.1016/j.heliyon.2022.e11976

[13] N. Khan et.al., 2018, A variable control chart under the truncated life test for Weibull distribution, Technologies, 6(2), 2-10. doi: 10.3390/technologies6020055

[14] N. Khan et.al., 2017, A mixed control chart adapted to the truncated life test based on the Weibull distribution. Operations Research and Decisions, 27, 43–55. doi: 10.5277/ord170103

[15] M. S. Aldosari, M. Aslam, C. H. Jun, 2017, A new attribute control chart using multiple dependent state repetitive sampling, IEEE Access, 5(3), 6192–6197. doi:10.1109/access.2017.2687523

[16] M. Aslam, O. H. Arif, C. H. Jun, 2016, An Attribute Control Chart Based on the Birnbaum-Saunders Distribution Using Repetitive Sampling. In IEEE Access; IEEE:Washington, DC, USA.

[17] S. Balamurali, P. Jeyadurga, 2019, An attribute np control chart for monitoring mean life using multiple deferred state sampling based on truncated life tests, International Journal of Reliability, Quality and Safety Engineering, 26(01), 1950004. doi: 10.1142/S0218539319500049

[18] B. Gokila, A. Sheik Abdullah, 2025, An attribute control chart approach for life testing using Exponential-Poisson distribution, Reliability: Theory & Applications, 20(2 (84)), 727–735. doi:10.24412/1932-2321-2025-489-370-380

[19] B. Gokila, A. Sheik Abdullah, 2025, Reliability based an attribute control chart using exponentiated exonential Poisson distribution under hybrid censoring. Reliability: Theory & Applications, *20*(3 (86)), 829-840.

[20] M. Gunasekaran, 2024, A new attribute control chart based on exponentiated exponential distribution under accelerated life test with hybrid censoring, Reliability: Theory & Applications,4:80(19): 850–860.

[21] B. S. Rao, M. R. Reddy, K. Rosaiah, 2023, An attribute control chart for time truncated life tests using exponentiated inverse Kumaraswamy distribution. Reliability: Theory & Applications,3(74), 206-217.

[22] T. Kavitha, M. Gunasekaran, 2020, Construction of control chart based on exponentiated exponential distribution, Journal of Engineering Sciences,11(4), 979- 985.

[23] R. Nagaraju, M. Palanivel, G. V. Sriramachandran, 2025, Development of an attribute control chart based on the Inverse Kumaraswamy distribution, Reliability: Theory & Applications, 2, 84(20), 372 – 381.

[24] G. S. Rao, 2018, A control chart for time truncated life tests using exponentiated half logistic distribution, Applied Mathematics Information Sciences, 12(1), 125-131. doi: 10.18576/amis/120111

[25] K. Rosaiah, G. S. Rao, M. S. Babu, 2018, MS. An attribute control chart under truncated life tests for the exponentiated Fréchet distribution, Quality Access to Success, 19(163), 47-51.

[26] K. Rosaiah et al., 2021, A control chart for time truncated life tests using Type-II generalized log-logistic distribution, Biometrics and Biostatistics International Journal, 10(4), 138–143. doi: 10.15406/bbij.2021.10.00340

[27] G. S. Rao, M. E. Paul, 2020, Time truncated control chart using loglogistic distribution, Biometrics and Biostatistics International Journal, 9, 76- 82. doi: 10.15406/BBIJ.2020.09.00303

[28] G. S. Rao, A. K. Fulment, P. K. Josephat, 2019, Attribute control chart for the Dagum distribution under truncated life tests. Life Cycle Reliability and Safety Engineering, 8, 329– 33. doi:10.1007/s41872-019-00090-3

[29] H. Tripathi, M. Saha, J. Tushaveera, 2022, Time truncated attribute control chart for generalized half normal distribution and its application, Life Cycle Reliab Safety Eng, 11(3), 229–235. doi: 10.1007/s41872-022-00195-2

[30] M. Aslam, N. Khan, C. H. Jun, 2016, A control chart for time truncated life tests using Pareto distribution of second kind, Journal of Statistical Computation and Simulation, 86 (11), 2113-2122. doi: 10.1080/00949655.2015.1103737

[31] A. Hag, H.W. Woodall, H. S. Steiner, 2025, A study of attribute control charts for censored lifetime data. Quality Engineering, 37(2):247-256. doi: 10.1080/08982112.2024.2375612

[32] N. S. Qutb, E. Rajhi, 2016, Estimation of the parameters of compound Weibull distribution, Journal of Mathematics, 12(4), 11-18. doi:10.9790/5728-1204021118

[33] R Core Team. (2025). *R: A language and environment for statistical computing* (Version 4.5.0). R Foundation for Statistical Computing. Vienna, Austria. https://www.R-project.org/